# Two-Photon Exclusive Production of Fully-Charmed Tetraquarks at the LHC

**Longjie Chen**, Wolfgang Schäfer, Antoni Szczurek

IFJ PAN

arXiv:2605.22500

June 14, 2026

THE HENRYK NIEWODNICZAŃSKI
INSTITUTE OF NUCLEAR PHYSICS
POLISH ACADEMY OF SCIENCES

NARODOWE CENTRUM NAUKI

# Outline

# Introduction

# Motivation: The $X(6900)$ and its family

- Observation of $X(6900) \to J/\psi J/\psi$ by LHCb , confirmed by ATLAS and CMS, established the existence of fully-charmed tetraquark states $T_{4c}$.

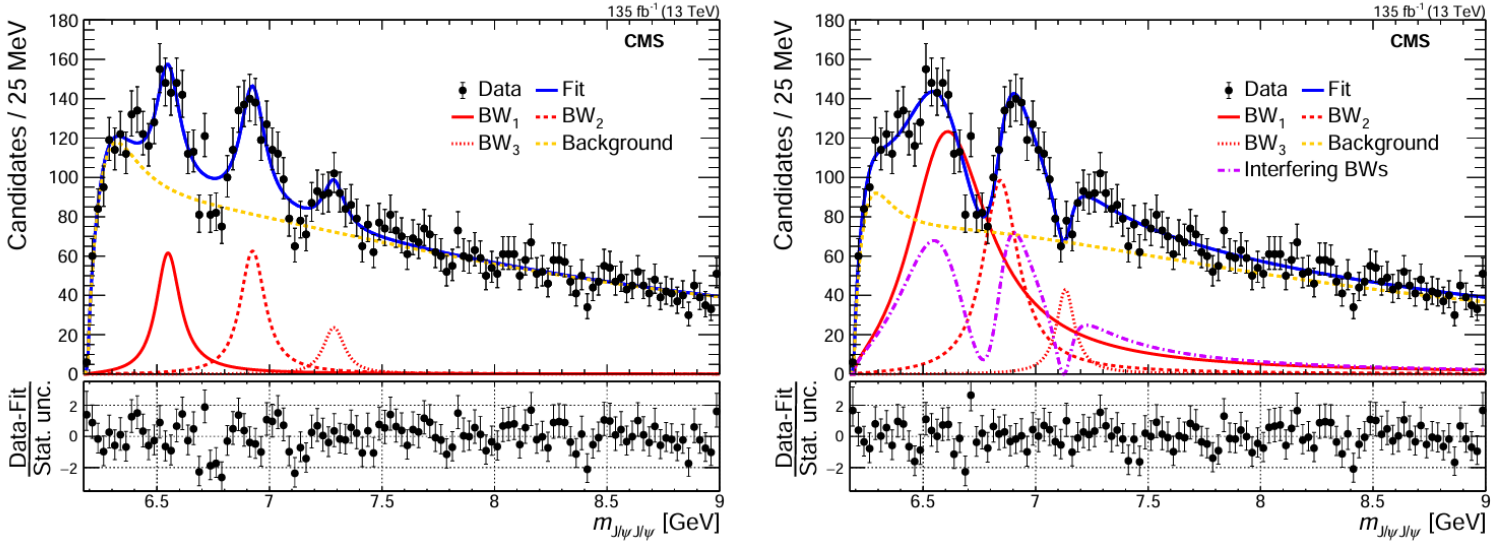


A. Hayrapetyan *et al.*, the $J/\psi J/\psi$ invariant mass spectrum.

# Motivation: The $X(6900)$ and its family

- Observation of $X(6900) \to J/\psi J/\psi$ by LHCb , confirmed by ATLAS and CMS, established the existence of fully-charmed tetraquark states $T_{4c}$.

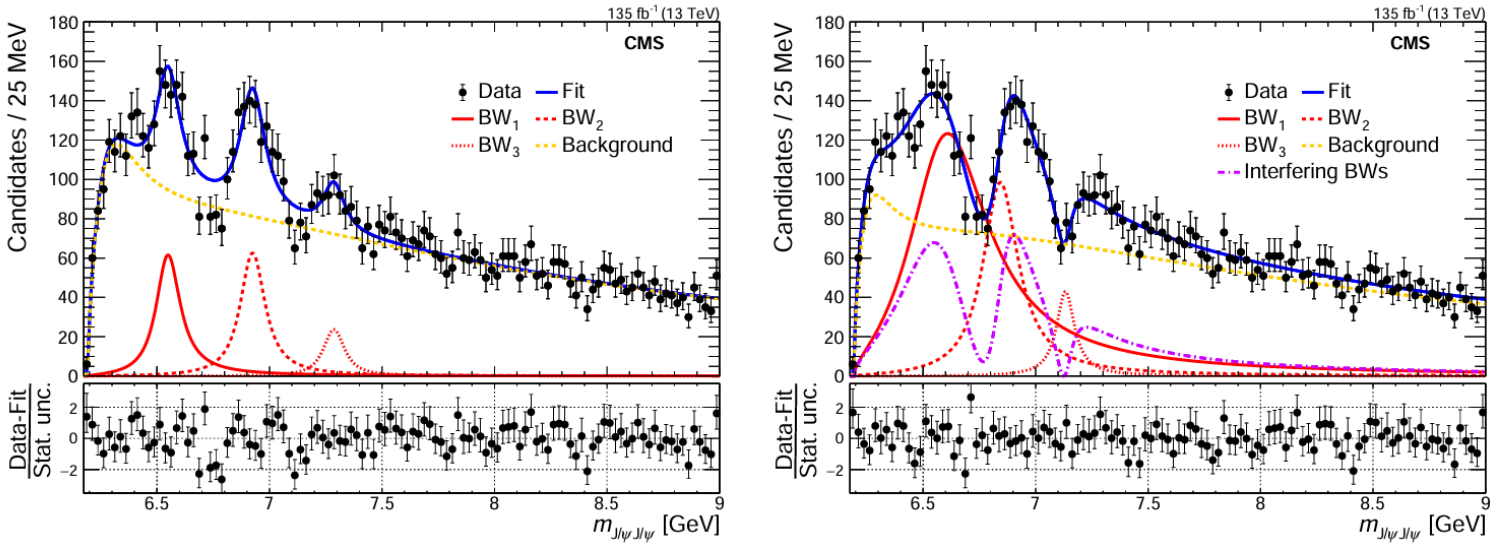


A. Hayrapetyan *et al.*, the $J/\psi J/\psi$ invariant mass spectrum.

- The leading interpretation is a compact diquark–antidiquark bound state.

# Motivation: The $X(6900)$ and its family

- Observation of $X(6900) \to J/\psi J/\psi$ by LHCb , confirmed by ATLAS and CMS, established the existence of fully-charmed tetraquark states $T_{4c}$.

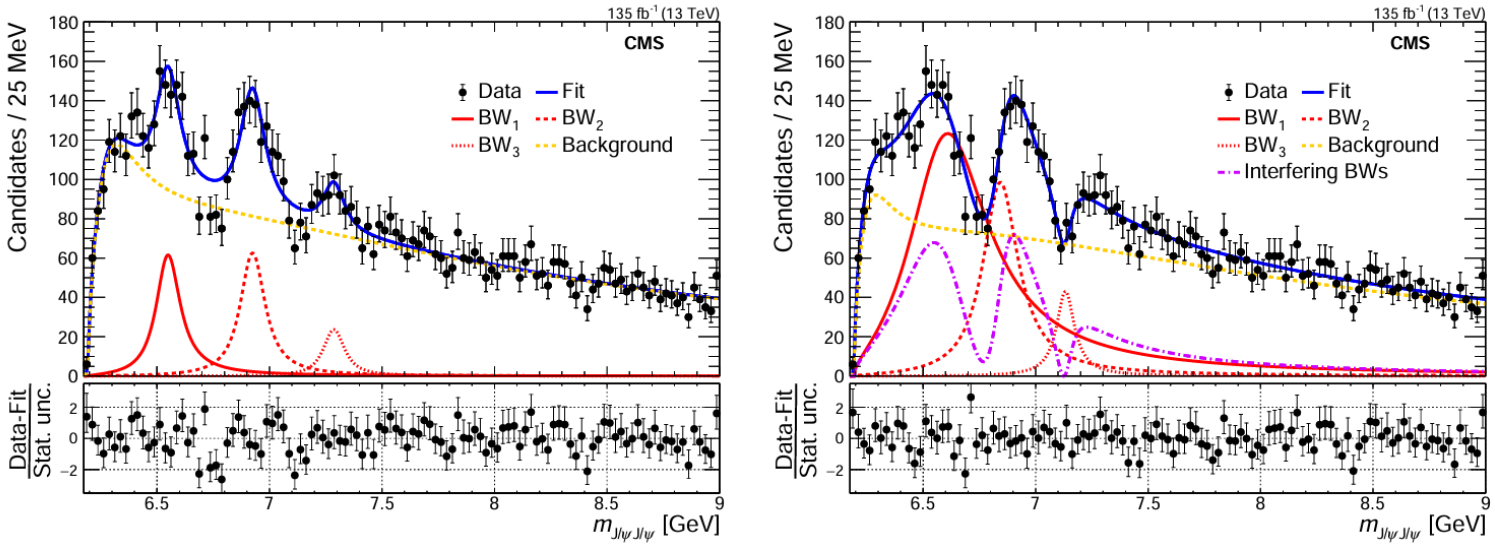


A. Hayrapetyan *et al.*, the $J/\psi J/\psi$ invariant mass spectrum.

- The leading interpretation is a compact diquark–antidiquark bound state.
- Recent CMS determination: $J^{PC} = 2^{++}$ for $X(6600)$ and $X(6900)$.

# Photon–Photon Fusion as a Clean Probe

- UPCs provide intense fluxes of quasi-real photons $\Rightarrow$ access $\gamma\gamma \to T_{4c}$.

# Photon–Photon Fusion as a Clean Probe

- UPCs provide intense fluxes of quasi-real photons $\Rightarrow$ access $\gamma\gamma \to T_{4c}$.
- Cross section is directly proportional to the two-photon decay width:

$$\sigma(\gamma\gamma \to T_{4c}) \propto \Gamma(T_{4c} \to \gamma\gamma)$$

# Photon–Photon Fusion as a Clean Probe

- UPCs provide intense fluxes of quasi-real photons $\Rightarrow$ access $\gamma\gamma \to T_{4c}$.
- Cross section is directly proportional to the two-photon decay width:

$$\sigma(\gamma\gamma \to T_{4c}) \propto \Gamma(T_{4c} \to \gamma\gamma)$$

- $\Gamma_{\gamma\gamma}$ is highly sensitive to the internal structure:
  - Compact tetraquark $\to$ calculable, $\mathcal{O}(0.1\text{–}1$ keV$)$.
  - Point-like diquark $\to$ much larger, $\mathcal{O}(10\text{–}100$ keV$)$.

# Photon–Photon Fusion as a Clean Probe

- UPCs provide intense fluxes of quasi-real photons $\Rightarrow$ access $\gamma\gamma \to T_{4c}$.
- Cross section is directly proportional to the two-photon decay width:

$$\sigma(\gamma\gamma \to T_{4c}) \propto \Gamma(T_{4c} \to \gamma\gamma)$$

- $\Gamma_{\gamma\gamma}$ is highly sensitive to the internal structure:
  - Compact tetraquark $\to$ calculable, $\mathcal{O}(0.1\text{–}1\ \text{keV})$.
  - Point-like diquark $\to$ much larger, $\mathcal{O}(10\text{–}100\ \text{keV})$.
- Some of the 40 tree-level diagrams for $\gamma\gamma \to c\bar{c}c\bar{c}$:

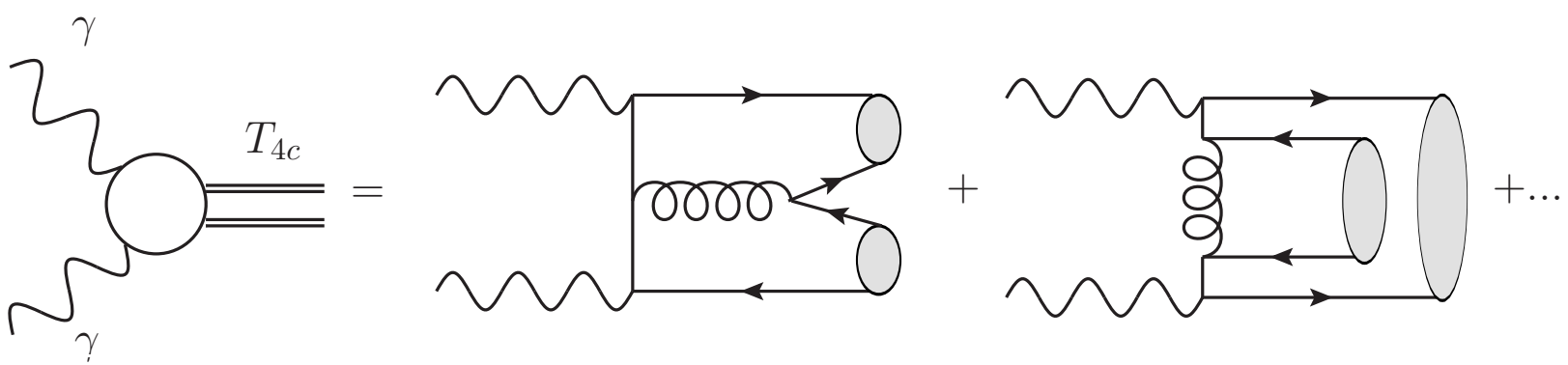

# Theoretical Framework

# NRQCD Factorisation

- We employ the Non-Relativistic QCD (NRQCD) effective field theory, which provides a rigorous expansion in $\alpha_s$ and the heavy-quark velocity $v$.

# NRQCD Factorisation

- We employ the Non-Relativistic QCD (NRQCD) effective field theory, which provides a rigorous expansion in $\alpha_s$ and the heavy-quark velocity $v$.
- NRQCD factorisation separates the decay amplitude into:

$$\mathcal{M}(\gamma\gamma \to T_{4c}) = \sum_n \mathcal{A}_n(\gamma\gamma \to c\bar{c}c\bar{c})\ \langle 0|\mathcal{O}_n|T_{4c}\rangle$$

# NRQCD Factorisation

- We employ the Non-Relativistic QCD (NRQCD) effective field theory, which provides a rigorous expansion in $\alpha_s$ and the heavy-quark velocity $v$.
- NRQCD factorisation separates the decay amplitude into:

$$\mathcal{M}(\gamma\gamma \to T_{4c}) = \sum_n \mathcal{A}_n(\gamma\gamma \to c\bar{c}c\bar{c})\ \langle 0|\mathcal{O}_n|T_{4c}\rangle$$

- Short-Distance Coefficients (SDCs):
  Perturbative $c\bar{c}c\bar{c} \to \gamma\gamma$ at the hard scale $\mu \sim 4m_c$, generated with FeynCalc.

# NRQCD Factorisation

- We employ the Non-Relativistic QCD (NRQCD) effective field theory, which provides a rigorous expansion in $\alpha_s$ and the heavy-quark velocity $v$.
- NRQCD factorisation separates the decay amplitude into:

$$\mathcal{M}(\gamma\gamma \to T_{4c}) = \sum_n \mathcal{A}_n(\gamma\gamma \to c\bar{c}c\bar{c})\ \langle 0|\mathcal{O}_n|T_{4c}\rangle$$

- Short-Distance Coefficients (SDCs):
  Perturbative $c\bar{c}c\bar{c} \to \gamma\gamma$ at the hard scale $\mu \sim 4m_c$, generated with FeynCalc.

  We calculate these at Leading Order (LO) in $\alpha_s$.

# NRQCD Factorisation

- We employ the Non-Relativistic QCD (NRQCD) effective field theory, which provides a rigorous expansion in $\alpha_s$ and the heavy-quark velocity $v$.
- NRQCD factorisation separates the decay amplitude into:

$$\mathcal{M}(\gamma\gamma \to T_{4c}) = \sum_n \mathcal{A}_n(\gamma\gamma \to c\bar{c}c\bar{c})\ \langle 0|\mathcal{O}_n|T_{4c}\rangle$$

- Short-Distance Coefficients (SDCs):
  Perturbative $c\bar{c}c\bar{c} \to \gamma\gamma$ at the hard scale $\mu \sim 4m_c$, generated with FeynCalc.

  We calculate these at Leading Order (LO) in $\alpha_s$.
- Long-Distance Matrix Elements (LDMEs):
  Non-perturbative, universal matrix elements of 4-quark NRQCD operators that parametrize the hadronization dynamics.

# NRQCD Factorisation

- We employ the Non-Relativistic QCD (NRQCD) effective field theory, which provides a rigorous expansion in $\alpha_s$ and the heavy-quark velocity $v$.
- NRQCD factorisation separates the decay amplitude into:

$$\mathcal{M}(\gamma\gamma \to T_{4c}) = \sum_n \mathcal{A}_n(\gamma\gamma \to c\bar{c}c\bar{c})\ \langle 0|\mathcal{O}_n|T_{4c}\rangle$$

- Short-Distance Coefficients (SDCs):
  Perturbative $c\bar{c}c\bar{c} \to \gamma\gamma$ at the hard scale $\mu \sim 4m_c$, generated with FeynCalc.

  We calculate these at Leading Order (LO) in $\alpha_s$.
- Long-Distance Matrix Elements (LDMEs):
  Non-perturbative, universal matrix elements of 4-quark NRQCD operators that parametrize the hadronization dynamics.

  Extracted from four-body wave functions at the origin.

# Diquark Operators and Colour Configurations

- Assume S-wave diquark–antidiquark structure. According to the Pauli principle we can have the following diquarks:

$$D_{kl} = S_{kl,rs}\, \psi_r^T i\sigma_2 \psi_s \quad \text{(spin-0, colour } \mathbf{6}\text{)},$$
$$D^j_{kl} = A_{kl,rs}\, \psi_r^T i\sigma_2 \sigma^j \psi_s \quad \text{(spin-1, colour } \bar{\mathbf{3}}\text{)}.$$

# Diquark Operators and Colour Configurations

- Assume S-wave diquark–antidiquark structure. According to the Pauli principle we can have the following diquarks:

$$D_{kl} = S_{kl,rs}\,\psi_r^T i\sigma_2 \psi_s \quad \text{(spin-0, colour } \mathbf{6}\text{)},$$
$$D^j_{kl} = A_{kl,rs}\,\psi_r^T i\sigma_2 \sigma^j \psi_s \quad \text{(spin-1, colour } \bar{\mathbf{3}}\text{)}.$$

- Tetraquark operators:

$$\mathcal{O}^{(0)}_{6\otimes\bar{6}} = D_{kl}\bar{D}_{kl}, \qquad \mathcal{O}^{(0)}_{\bar{3}\otimes 3} = \tfrac{1}{\sqrt{3}}\delta_{ij} D^i_{kl}\bar{D}^j_{kl},$$
$$\mathcal{O}^{(2)}_{\bar{3}\otimes 3} = E^*_{ij}(J_z) D^i_{kl}\bar{D}^j_{kl}.$$

# Diquark Operators and Colour Configurations

- Assume S-wave diquark–antidiquark structure. According to the Pauli principle we can have the following diquarks:

$$D_{kl} = S_{kl,rs}\,\psi_r^T i\sigma_2 \psi_s \quad \text{(spin-0, colour } \mathbf{6}\text{)},$$
$$D^j_{kl} = A_{kl,rs}\,\psi_r^T i\sigma_2 \sigma^j \psi_s \quad \text{(spin-1, colour } \bar{\mathbf{3}}\text{)}.$$

- Tetraquark operators:

$$\mathcal{O}^{(0)}_{6\otimes\bar{6}} = D_{kl}\bar{D}_{kl}, \qquad \mathcal{O}^{(0)}_{\bar{3}\otimes 3} = \tfrac{1}{\sqrt{3}}\delta_{ij} D^i_{kl}\bar{D}^j_{kl},$$
$$\mathcal{O}^{(2)}_{\bar{3}\otimes 3} = E^*_{ij}(J_z) D^i_{kl}\bar{D}^j_{kl}.$$

- For the scalar ($0^{++}$): both $\bar{3}\otimes 3$ and $6\otimes\bar{6}$ contribute and mix.
- For the tensor ($2^{++}$): only $\bar{3}\otimes 3$ (spin-1 diquarks, S-wave).

# Extracted Short-Distance Coefficients

- The factorised amplitudes $F_{TT}$, $F_{TT,0}$, $F_{TT,2}$ relating SDCs to LDMEs are given in the backup. Matching at LO yields the SDCs:

$$\tilde{F}_{TT,0} = \frac{4\pi\alpha_s e_Q^2}{\sqrt{3}\, m_Q^4}, \qquad \tilde{F}_{TT,2} = \frac{128\pi\alpha_s e_Q^2}{\sqrt{3}\, m_Q^2},$$

$$\tilde{F}_{TT}^{66} = -\frac{8\sqrt{2}\pi\alpha_s e_Q^2}{\sqrt{3}\, m_Q^2}, \qquad \tilde{F}_{TT}^{33} = \frac{48\pi\alpha_s e_Q^2}{m_Q^2}.$$

# Extracted Short-Distance Coefficients

- The factorised amplitudes $F_{TT}$, $F_{TT,0}$, $F_{TT,2}$ relating SDCs to LDMEs are given in the backup. Matching at LO yields the SDCs:

$$\tilde{F}_{TT,0} = \frac{4\pi\alpha_s e_Q^2}{\sqrt{3}\, m_Q^4}, \qquad \tilde{F}_{TT,2} = \frac{128\pi\alpha_s e_Q^2}{\sqrt{3}\, m_Q^2},$$

$$\tilde{F}_{TT}^{66} = -\frac{8\sqrt{2}\pi\alpha_s e_Q^2}{\sqrt{3}\, m_Q^2}, \qquad \tilde{F}_{TT}^{33} = \frac{48\pi\alpha_s e_Q^2}{m_Q^2}.$$

- Decay widths in terms of LDMEs:

$$\Gamma(2^{++} \to \gamma\gamma) = \frac{128\pi^3\alpha_{em}^2\alpha_s^2 e_Q^4}{15\, m_Q^8}\left[1 + \tfrac{1}{6}\left(\tfrac{M}{4m_Q}\right)^4\right]\left|\langle \mathcal{O}^{(2)}_{\bar{3}\otimes 3}\rangle\right|^2,$$

$$\Gamma(0^{++} \to \gamma\gamma) = \frac{\pi^3\alpha_{em}^2\alpha_s^2 e_Q^4}{m_Q^8}\Big[18|\langle \mathcal{O}_{\bar{3}3}\rangle|^2 + \tfrac{1}{3}|\langle \mathcal{O}_{6\bar{6}}\rangle|^2 - 2\sqrt{6}\ \mathrm{Re}\big(\langle \mathcal{O}_{\bar{3}3}\rangle\langle \mathcal{O}_{6\bar{6}}\rangle^*\big)\Big].$$

# Calculation & Inputs

# Inputs I: Running of $\alpha_s$

- 2-loop RG evolution with RunDec.
- Flavour thresholds:
  $\alpha_s^{(5)}(m_Z) \to \alpha_s^{(5)}(m_b) \to \alpha_s^{(4)}(m_b) \to \alpha_s^{(4)}(m_c) \to \alpha_s^{(3)}(m_c)$.

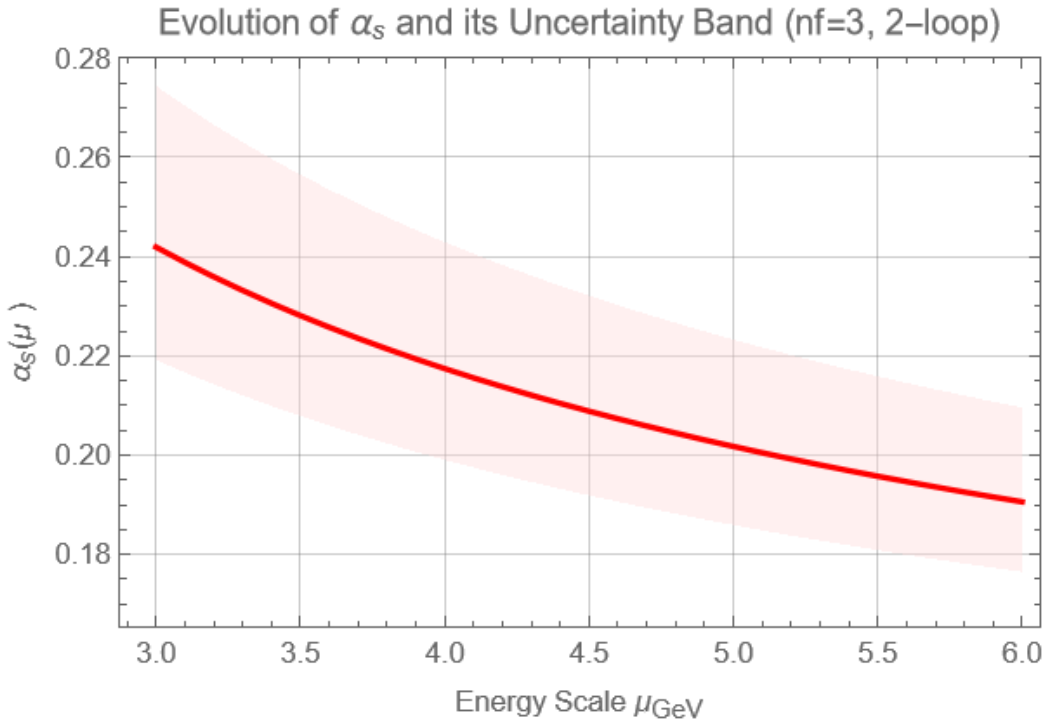


Figure: $\alpha_s(\mu)$ in the $n_f = 3$ theory.

- Central scale $\mu_0 = 3$ GeV $\simeq 2m_c$.
- Scale variation $\mu \in [2m_c, 4m_c]$ estimates theory uncertainty ($\sim 30\%$).

# Inputs II: Wave Functions at the Origin

- LDMEs extracted from 4-body wave functions, obtained via the **Gaussian Expansion Method** applied to the extended relativized quark model from Q. F. Lü, D. Y. Chen and Y. B. Dong, "Masses of fully heavy tetraquarks $QQ\bar{Q}\bar{Q}$ in an extended relativized quark model," Eur. Phys. J. C **80** (2020) no.9, 871
- For scalar states: colour mixing leads to two physical eigenstates.

| Mass ($J^{PC}$) | State | Eigenvector | $\psi_{\bar{3}3}(0)$ | $\psi_{6\bar{6}}(0)$ | $\psi_{\text{phys}}(0)$ |
|---|---|---|---|---|---|
| 6435 ($0^{++}$) | 1s | [0.62, 0.79] | 0.0466 | 0.0283 | 0.0510 |
| 6542 ($0^{++}$) | 1s | [0.79, -0.62] | 0.0466 | 0.0283 | 0.0189 |
| 6849 ($0^{++}$) | 2s | [0.50, 0.87] | 0.0721 | 0.0466 | 0.0764 |
| 6940 ($0^{++}$) | 2s | [0.87, -0.50] | 0.0721 | 0.0466 | 0.0391 |
| 6543 ($2^{++}$) | 1s | 1 | 0.0300 | — | 0.0300 |
| 6928 ($2^{++}$) | 2s | 1 | 0.0471 | — | 0.0471 |

- Note: $\psi(0)$ of $2s$ states is larger than $1s$ – counterintuitive! For $3s$, $\psi(0) \simeq 0$.

# Results & Discussion

# Predictions for $\Gamma(T_{4c} \to \gamma\gamma)$

- We identify: $X(6600) \equiv (2^{++}, 1s)$, $X(6900) \equiv (2^{++}, 2s)$, $X(7100) \equiv (2^{++}, 3s)$.

| Mass $(J^{PC})$ | State | Description | $\Gamma_{\gamma\gamma}$ (keV) |
|---|---|---|---|
| 6435 $(0^{++})$ | 1s | Mixture 1 (ground) | $0.106^{+0.03}_{-0.02}$ |
| 6542 $(0^{++})$ | 1s | Mixture 2 (ground) | $0.245^{+0.07}_{-0.05}$ |
| **6849 $(0^{++})$** | **2s** | **Mixture 1 (radial)** | $\mathbf{0.149^{+0.05}_{-0.03}}$ |
| **6940 $(0^{++})$** | **2s** | **Mixture 2 (radial)** | $\mathbf{0.688^{+0.21}_{-0.15}}$ |
| 6543 $(2^{++})$ | 1s | $X(6600)$ | $0.088^{+0.03}_{-0.02}$ |
| **6928 $(2^{++})$** | **2s** | $\boldsymbol{X(6900)}$ | $\mathbf{0.217^{+0.07}_{-0.05}}$ |

- The $X(7100)$ candidate, identified with $(2^{++}, 3s)$, has vanishing $\Gamma_{\gamma\gamma}$.
- $\Gamma_{\gamma\gamma}$ spans 0.1–0.7 keV. Uncertainties dominated by scale variation.

# Comparison with Literature

- Our results: $\mathcal{O}(0.1\text{–}0.7$ keV). The literature spans an enormous range.

| **Approach** | **Reference** | $\Gamma_{\gamma\gamma}$ (keV) | Note |
|---|---|---|---|
| Quark model (1987) | Badalian et al. | $\sim 10^{-3}$ | $10^{-4}\,\Gamma(\eta_c \to \gamma\gamma)$ |
| NRQCD (this work) | **This work** | $\mathbf{0.1\text{–}0.7}$ | LDMEs from GEM wave fns. |
| NRQCD LO+NLO | Sang et al. / Liu et al. | $0.1\text{–}0.5$ | Similar ballpark |
| VDM | Esposito et al. | $0.086 \times B_\psi$ | $B_\psi \sim 1 \Rightarrow 0.086$ |
| Point-Like Diquark | Kalamidas et al. | $\mathbf{5\text{–}82}$ | Two orders larger |
| LbL fit | Biloshytskyi et al. | $45\text{–}67$ | Spin-0 only |

- The point-like diquark model overestimates by $\sim 2$ orders of magnitude – treats diquarks as elementary fields.
- VDM model implicitly assumes $B_\psi \equiv \mathrm{Br}(T_{4c} \to J/\psi J/\psi) \sim \mathcal{O}(1)$. However model calculations of decays and hadronic production rather suggest $B_\psi \sim \mathcal{O}(10^{-3})$.

# Phenomenology: UPCs

# Two mechanisms for $T_{4c}$ production in UPCs

We discuss two different final states $J/\psi J/\psi$ and $\gamma\gamma$ through which fully-charmed tetraquarks can be accessed in $AA$ ultraperipheral collisions. Both final states receive direct continuum *and* resonant contributions:

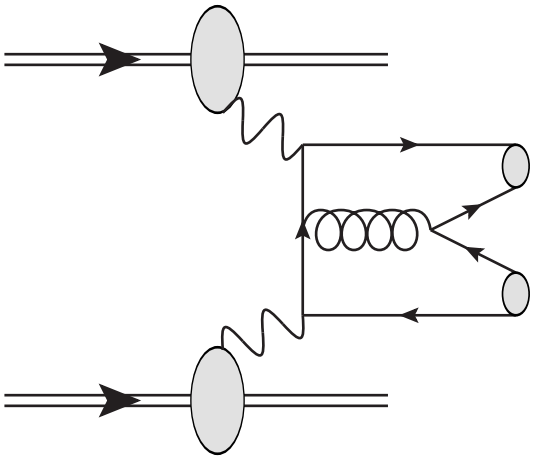

(a) : $\gamma\gamma \to J/\psi J/\psi$ and $\gamma\gamma \to \gamma\gamma$.

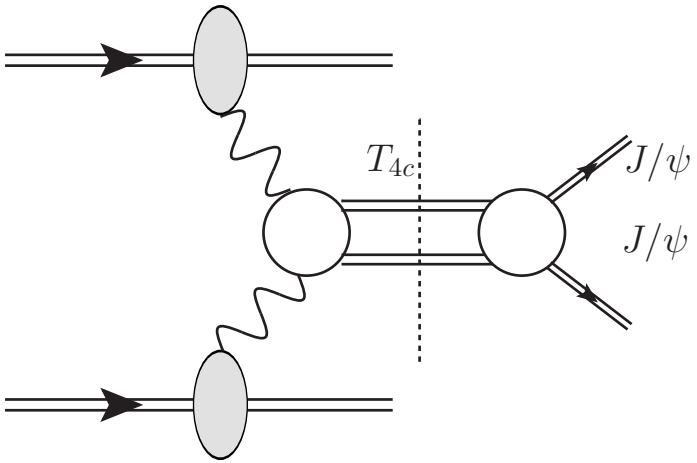


(b) : $\gamma\gamma \to T_{4c} \to J/\psi\, J/\psi$ and $\gamma\gamma \to T_{4c} \to \gamma\gamma$.

# Two mechanisms for $T_{4c}$ production in UPCs

We discuss two different final states $J/\psi J/\psi$ and $\gamma\gamma$ through which fully-charmed tetraquarks can be accessed in $AA$ ultraperipheral collisions. Both final states receive direct continuum *and* resonant contributions:

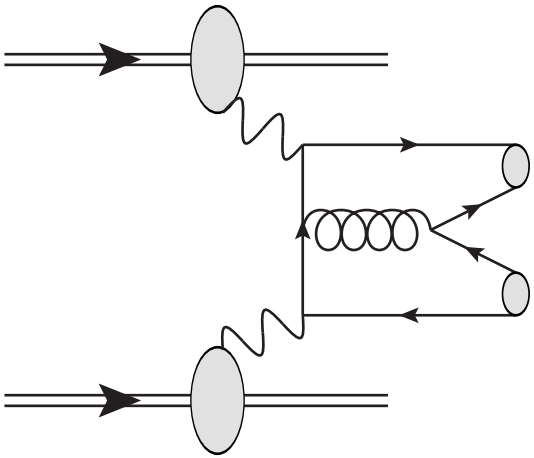

(a) : $\gamma\gamma \to J/\psi J/\psi$ and $\gamma\gamma \to \gamma\gamma$.

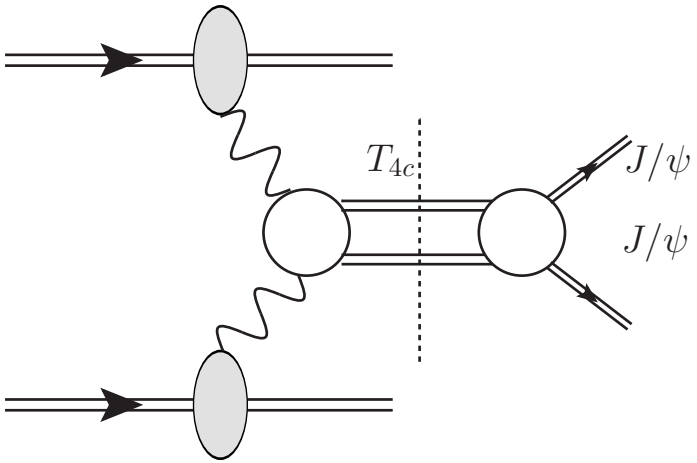


(b) : $\gamma\gamma \to T_{4c} \to J/\psi\, J/\psi$ and $\gamma\gamma \to T_{4c} \to \gamma\gamma$.

- The direct $\gamma\gamma \to \gamma\gamma$ continuum is the QED light-by-light box diagram.
- The direct $\gamma\gamma \to J/\psi J/\psi$ continuum is computed in LO NRQCD.

# Two mechanisms for $T_{4c}$ production in UPCs

We discuss two different final states $J/\psi J/\psi$ and $\gamma\gamma$ through which fully-charmed tetraquarks can be accessed in $AA$ ultraperipheral collisions. Both final states receive direct continuum *and* resonant contributions:

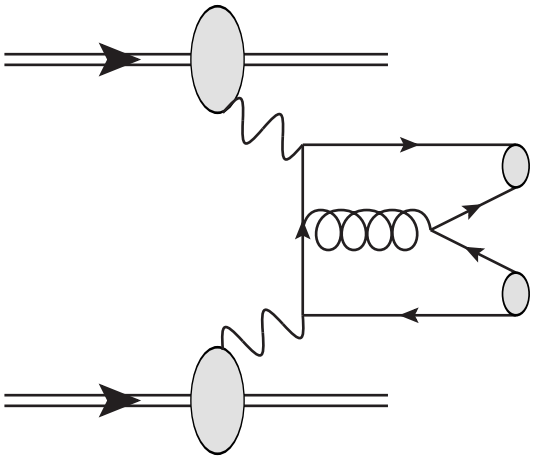

(a) : $\gamma\gamma \to J/\psi J/\psi$ and $\gamma\gamma \to \gamma\gamma$.

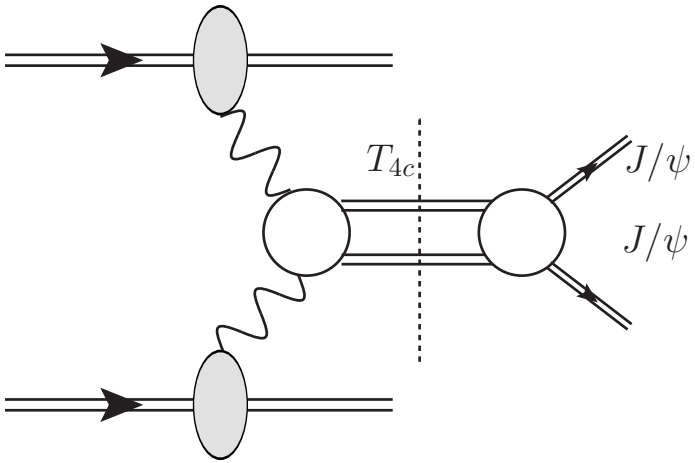


(b) : $\gamma\gamma \to T_{4c} \to J/\psi\, J/\psi$ and $\gamma\gamma \to T_{4c} \to \gamma\gamma$.

- The direct $\gamma\gamma \to \gamma\gamma$ continuum is the QED light-by-light box diagram.
- The direct $\gamma\gamma \to J/\psi J/\psi$ continuum is computed in LO NRQCD.
- The resonant contributions scale as $\Gamma_{\gamma\gamma} \times B_\psi$ (for $J/\psi J/\psi$) and $\Gamma^2_{\gamma\gamma}/\Gamma_{\rm tot}$ (for $\gamma\gamma$).

# $T_{4c}$ Production in UPCs

- The UPC cross section is:

$$\sigma(AA \to T_{4c}AA) = \int dW^2 \, \frac{d\mathcal{L}_{\gamma\gamma}}{dW^2} \, \sigma(\gamma\gamma \to T_{4c}; W)$$

- Photon–photon luminosity is given in terms of the Weizsäcker–Williams fluxes of photons as

$$\frac{d\mathcal{L}_{\gamma\gamma}}{dW^2} = \int \frac{dx_1}{x_1} \frac{dx_2}{x_2} \delta(W^2 - x_1 x_2 s_{\rm NN}) \int d^2\boldsymbol{b}_1 d^2\boldsymbol{b}_2 \, S^2(|\boldsymbol{b}_1 - \boldsymbol{b}_2|) N(x_1, \boldsymbol{b}_1) N(x_2, \boldsymbol{b}_2),$$

# $T_{4c}$ Production in UPCs

- The UPC cross section is:

$$\sigma(AA \to T_{4c}AA) = \int dW^2 \, \frac{d\mathcal{L}_{\gamma\gamma}}{dW^2} \, \sigma(\gamma\gamma \to T_{4c}; W)$$

- Photon–photon luminosity is given in terms of the Weizsäcker–Williams fluxes of photons as

$$\frac{d\mathcal{L}_{\gamma\gamma}}{dW^2} = \int \frac{dx_1}{x_1} \frac{dx_2}{x_2} \delta(W^2 - x_1 x_2 s_{\rm NN}) \int d^2\boldsymbol{b}_1 d^2\boldsymbol{b}_2 \, S^2(|\boldsymbol{b}_1 - \boldsymbol{b}_2|) N(x_1, \boldsymbol{b}_1) N(x_2, \boldsymbol{b}_2),$$

- Partonic cross section: Breit–Wigner form

$$\sigma(\gamma\gamma \to T_{4c}(J); W) = 8\pi(2J+1)\frac{M}{W} \, \frac{\Gamma_{\rm tot}\,\Gamma_{\gamma\gamma}}{(W^2 - M^2)^2 + M^2\Gamma_{\rm tot}^2}$$

# $T_{4c}$ Production in UPCs

- The UPC cross section is:

$$\sigma(AA \to T_{4c}AA) = \int dW^2 \, \frac{d\mathcal{L}_{\gamma\gamma}}{dW^2} \, \sigma(\gamma\gamma \to T_{4c}; W)$$

- Photon–photon luminosity is given in terms of the Weizsäcker–Williams fluxes of photons as

$$\frac{d\mathcal{L}_{\gamma\gamma}}{dW^2} = \int \frac{dx_1}{x_1}\frac{dx_2}{x_2}\delta(W^2 - x_1 x_2 s_{\rm NN}) \int d^2\boldsymbol{b}_1 d^2\boldsymbol{b}_2 \, S^2(|\boldsymbol{b}_1 - \boldsymbol{b}_2|) N(x_1, \boldsymbol{b}_1) N(x_2, \boldsymbol{b}_2),$$

- Partonic cross section: Breit–Wigner form

$$\sigma(\gamma\gamma \to T_{4c}(J); W) = 8\pi(2J+1)\frac{M}{W} \, \frac{\Gamma_{\rm tot}\,\Gamma_{\gamma\gamma}}{(W^2 - M^2)^2 + M^2\Gamma_{\rm tot}^2}$$

- Total widths: $\Gamma_{\rm tot} = 0.446$ GeV for $X(6600)$, $0.135$ GeV for $X(6900)$[arXiv: 2602.02252], $0.1$ GeV for others.

# Total Cross Sections in $^{208}Pb + ^{208}Pb$ UPC, $\sqrt{s_{NN}} = 5.5\,\mathrm{TeV}$

| Mass (MeV) | $J^{PC}$ | State | $\sigma(\gamma\gamma \to T_{4c})$ (nb) | $\sigma(AA \to T_{4c}AA)$ ($\mu$b) |
|---|---|---|---|---|
| 6435 | $0^{++}$ | 1s | 0.251 | 0.351 |
| 6542 | $0^{++}$ | 1s | 0.560 | 0.769 |
| 6849 | $0^{++}$ | 2s | 0.311 | 0.396 |
| 6940 | $0^{++}$ | 2s | 1.398 | 1.738 |
| 6543 | $2^{++}$ | 1s | 1.006 | 1.164 |
| **6928** | $\mathbf{2^{++}}$ | **2s** | **2.212** | **2.733** |

- Tensor states profit from $(2J+1) = 5$ spin factor.
- Total $\sigma(AA \to T_{4c}AA) \sim \mu$b; must be compared with UPC luminosities of a few nb$^{-1}$.

# $J/\psi J/\psi$ Channel

- Simplified $T_{4c} \to J/\psi J/\psi$ couplings (following Esposito et al.):

$$\langle T_{4c}(0^{++})|V_1V_2\rangle = \alpha_0\, \varepsilon_1\cdot\varepsilon_2, \quad \langle T_{4c}(2^{++})|V_1V_2\rangle = \alpha_2\, E_{\mu\nu}\, \varepsilon_1^{\mu}\varepsilon_2^{\nu}.$$

# $J/\psi J/\psi$ Channel

- Simplified $T_{4c} \to J/\psi J/\psi$ couplings (following Esposito et al.):

$$\langle T_{4c}(0^{++})|V_1V_2\rangle = \alpha_0\, \varepsilon_1\cdot\varepsilon_2, \quad \langle T_{4c}(2^{++})|V_1V_2\rangle = \alpha_2\, E_{\mu\nu}\, \varepsilon_1^{\mu}\varepsilon_2^{\nu}.$$

- The continuum $\gamma\gamma \to J/\psi J/\psi$ is computed in LO NRQCD with $\mathrm{B}_\psi = 3\times 10^{-3}, |\psi(0)|^2 = 0.08$ GeV$^3$, $m_c = 1.5$ GeV, $\alpha_s = 0.24$.

# $J/\psi J/\psi$ Channel

- Simplified $T_{4c} \to J/\psi J/\psi$ couplings (following Esposito et al.):

$$\langle T_{4c}(0^{++})|V_1V_2\rangle = \alpha_0\, \varepsilon_1\cdot\varepsilon_2, \quad \langle T_{4c}(2^{++})|V_1V_2\rangle = \alpha_2\, E_{\mu\nu}\, \varepsilon_1^{\mu}\varepsilon_2^{\nu}.$$

- The continuum $\gamma\gamma \to J/\psi J/\psi$ is computed in LO NRQCD with $\mathrm{B}_\psi = 3\times 10^{-3}, |\psi(0)|^2 = 0.08$ GeV$^3$, $m_c = 1.5$ GeV, $\alpha_s = 0.24$.

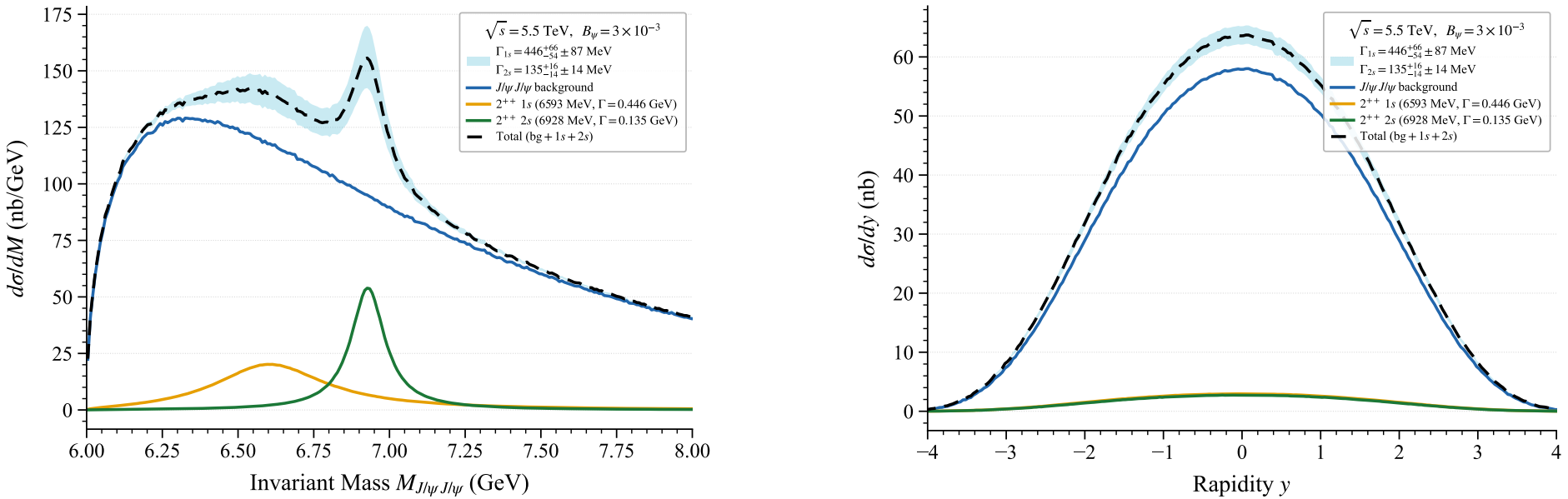


Invariant mass (left) and rapidity (right) for $J/\psi$ pairs, with $B_\psi = 3\times 10^{-3}$.

# $J/\psi J/\psi$ Channel

- Simplified $T_{4c} \to J/\psi J/\psi$ couplings (following Esposito et al.):

$$\langle T_{4c}(0^{++})|V_1V_2\rangle = \alpha_0\, \varepsilon_1\cdot\varepsilon_2, \quad \langle T_{4c}(2^{++})|V_1V_2\rangle = \alpha_2\, E_{\mu\nu}\, \varepsilon_1^{\mu}\varepsilon_2^{\nu}.$$

- The continuum $\gamma\gamma \to J/\psi J/\psi$ is computed in LO NRQCD with $\mathrm{B}_\psi = 3\times 10^{-3}$, $|\psi(0)|^2 = 0.08$ GeV$^3$, $m_c = 1.5$ GeV, $\alpha_s = 0.24$.

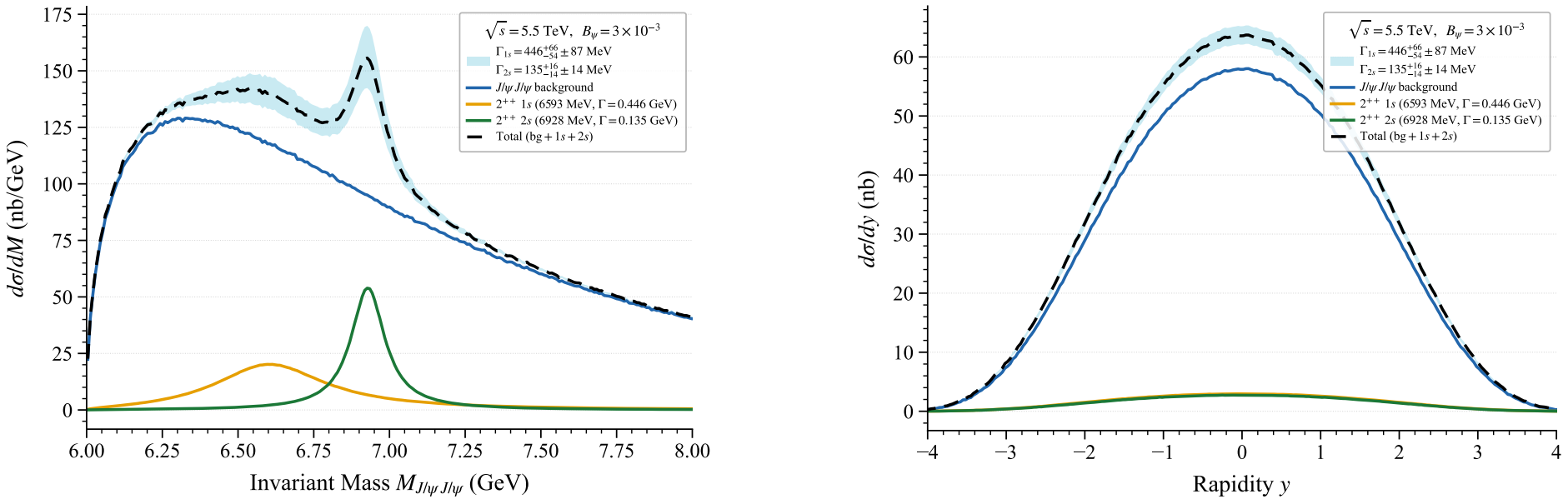


Invariant mass (left) and rapidity (right) for $J/\psi$ pairs, with $B_\psi = 3\times 10^{-3}$.

- The broad $1s$ (6593 MeV) spans 6.3–7.0 GeV; the narrow $2s$ (6928 MeV) forms a sharp peak.

# $J/\psi J/\psi$ Channel

- Simplified $T_{4c} \to J/\psi J/\psi$ couplings (following Esposito et al.):

$$\langle T_{4c}(0^{++})|V_1V_2\rangle = \alpha_0\, \varepsilon_1\cdot\varepsilon_2, \quad \langle T_{4c}(2^{++})|V_1V_2\rangle = \alpha_2\, E_{\mu\nu}\, \varepsilon_1^{\mu}\varepsilon_2^{\nu}.$$

- The continuum $\gamma\gamma \to J/\psi J/\psi$ is computed in LO NRQCD with $\mathrm{B}_\psi = 3\times 10^{-3}$, $|\psi(0)|^2 = 0.08$ GeV$^3$, $m_c = 1.5$ GeV, $\alpha_s = 0.24$.

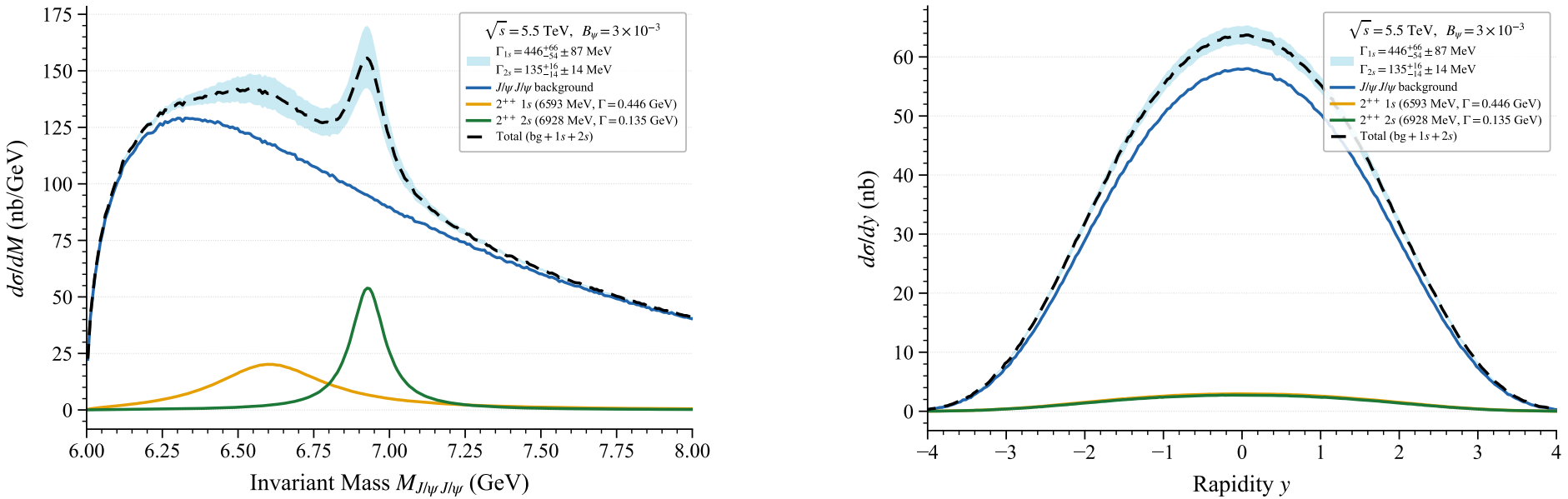


Invariant mass (left) and rapidity (right) for $J/\psi$ pairs, with $B_\psi = 3\times 10^{-3}$.

- The broad $1s$ (6593 MeV) spans 6.3–7.0 GeV; the narrow $2s$ (6928 MeV) forms a sharp peak.
- Resonant signal exceeds the continuum $\Rightarrow$ promising for HL-LHC.

# $\gamma\gamma$ Channel

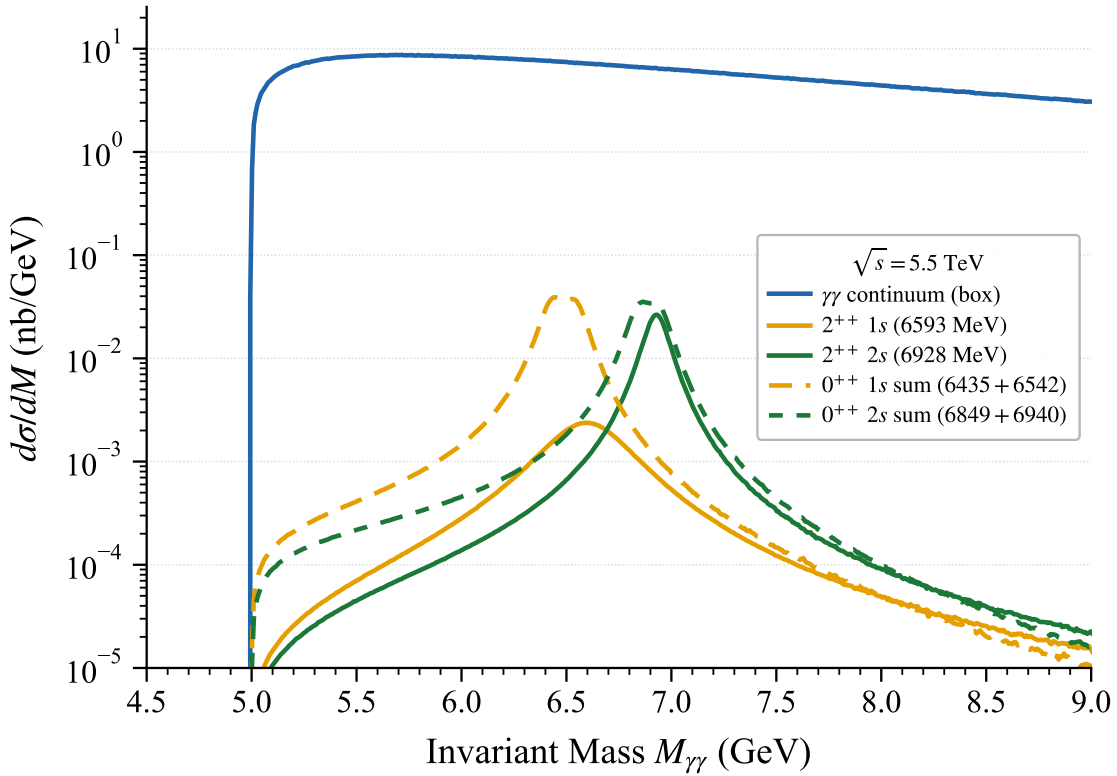


Figure: Diphoton invariant-mass distribution.

- QED box continuum dominates by $\sim 2$ orders of magnitude.

# $\gamma\gamma$ Channel

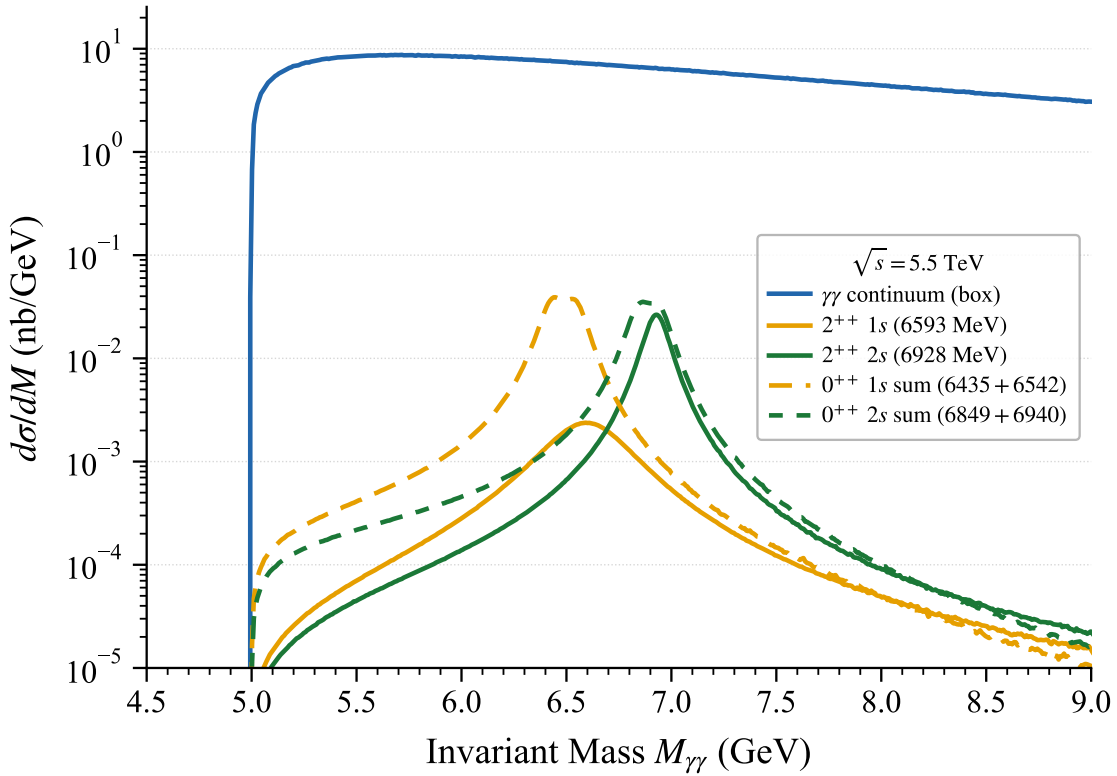


Figure: Diphoton invariant-mass distribution.

- QED box continuum dominates by $\sim 2$ orders of magnitude.
- All resonant contributions are at the level of a few $\times 10^{-2}$ nb.

# $\gamma\gamma$ Channel

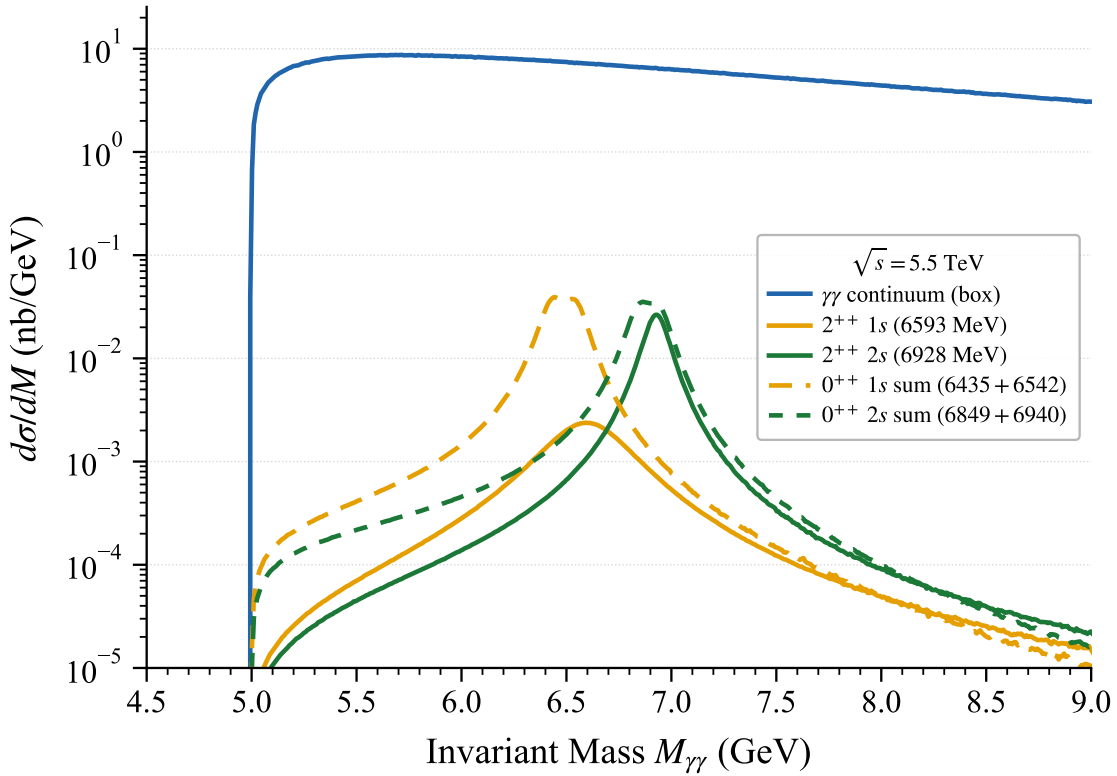


Figure: Diphoton invariant-mass distribution.

- QED box continuum dominates by $\sim 2$ orders of magnitude.
- All resonant contributions are at the level of a few $\times 10^{-2}$ nb.
- In clear disagreement with the VDM-based result of Biloshytskyi et al.

# Summary

# Summary and Outlook

## Summary

- Presented LO NRQCD predictions for $\Gamma(T_{4c} \to \gamma\gamma)$ of $0^{++}$ and $2^{++}$ states.
- LDMEs extracted from realistic 4-body wave functions (GEM).
- Key results: $\Gamma(2^{++}_{2s}) \approx 0.22$ keV, $\Gamma(0^{++}_{2s}) \approx 0.15$–$0.69$ keV.
- $J/\psi J/\psi$ channel: resonant signal exceeds continuum – promising.
- $\gamma\gamma$ channel: resonant contributions much smaller than continuum – contradicts VDM predictions.

# Summary and Outlook

## Summary

- Presented LO NRQCD predictions for $\Gamma(T_{4c} \to \gamma\gamma)$ of $0^{++}$ and $2^{++}$ states.
- LDMEs extracted from realistic 4-body wave functions (GEM).
- Key results: $\Gamma(2^{++}_{2s}) \approx 0.22$ keV, $\Gamma(0^{++}_{2s}) \approx 0.15$–$0.69$ keV.
- $J/\psi J/\psi$ channel: resonant signal exceeds continuum – promising.
- $\gamma\gamma$ channel: resonant contributions much smaller than continuum – contradicts VDM predictions.

## Outlook

- NLO calculation of SDCs needed to reduce $\sim 30\%$ scale uncertainty.
- Larger UPC luminosity at HL-LHC would be highly valuable.
- LDMEs can be used for other NRQCD-factorized processes.
- Matching between high $p_T$ regions and low $p_T$ regions in $pp$ collisions.

# Thank You!

# Backup: Four-Body Schrödinger Equation

- The LDMEs are determined by $|\psi(0)|^2$, obtained by solving the 4-body Schrödinger equation:

$$H = \sum_{i=1}^{4} \sqrt{p_i^2 + m_i^2} + \sum_{i<j} V_{ij}(\mathbf{r}_{ij}),$$

$$V_{ij} = \mathbf{F}_i \cdot \mathbf{F}_j \left[ V_{\text{conf}}(r_{ij}) + V_{\text{OGE}}(r_{ij}) \right].$$

- Solved via the **Gaussian Expansion Method** (GEM).
- Physical states obtained by diagonalising the Hamiltonian matrix $\Rightarrow$ colour mixing for scalars.

# Backup: Branching ratio $B_\psi$

- Total widths of the three $X \to J/\psi J/\psi$ peaks are known from CMS/LHCb, but $B_\psi$ is not measured.
- Two conflicting pictures in the literature:
  - Several early works (VDM, LbL fits) assume $B_\psi \sim \mathcal{O}(1)$ [Phys.Rev.D 104 (2021) 11, 114029,Phys.Rev.D 106 (2022) 11, L111902].
  - Ref. [Phys.Lett.B 811 (2020) 135952] evaluates the dimuon final states: $\mathcal{B}(T_{4c}(2^{++}) \to \mu^+\mu^-\mu^+\mu^-) \sim 10^{-5}$.
    Using $\mathcal{B}(J/\psi \to \mu^+\mu^-) \approx 0.06$, then obtain $B_\psi \sim 3 \times 10^{-3}$.
- Such small values are also required to explain the observed $pp$ event rates [JHEP 01 (2025) 093, arXiv:2510.02085]. , model calculations with larger $B_\psi \sim 10\%$ or more do exist [arXiv:2512.18569 ].
- Our choice: we adopt the representative value

$$B_\psi = 0.003$$

for *all* resonances, although $B_\psi$ may strongly depend on the state [Phys.Rev.D 109 (2024) 7, 076017].

# Backup: Analytic Results for SDCs

$$\tilde{F}_{TT,0} = \frac{4\pi\alpha_s e_Q^2}{\sqrt{3}\, m_Q^4}, \qquad \tilde{F}_{TT,2} = \frac{128\pi\alpha_s e_Q^2}{\sqrt{3}\, m_Q^2},$$

$$\tilde{F}_{TT}^{66} = -\frac{8\sqrt{2}\pi\alpha_s e_Q^2}{\sqrt{3}\, m_Q^2}, \qquad \tilde{F}_{TT}^{33} = \frac{48\pi\alpha_s e_Q^2}{m_Q^2}.$$

Decay width factorisation:

$$F_{TT} = \tilde{F}_{TT}^{66} \cdot \frac{\sqrt{2M}\langle \mathcal{O}^{(0)}_{6\otimes\bar{6}}\rangle}{4(2m_Q)^2} + \tilde{F}_{TT}^{33} \cdot \frac{\sqrt{2M}\langle \mathcal{O}^{(0)}_{\bar{3}\otimes 3}\rangle}{4(2m_Q)^2},$$

$$F_{TT,0} = \tilde{F}_{TT,0} \cdot \frac{\sqrt{2M}\langle \mathcal{O}^{(2)}_{\bar{3}\otimes 3}\rangle}{4(2m_Q)^2}, \quad F_{TT,2} = \tilde{F}_{TT,2} \cdot \frac{\sqrt{2M}\langle \mathcal{O}^{(2)}_{\bar{3}\otimes 3}\rangle}{4(2m_Q)^2}.$$

# Backup: Comparison of LDMEs ($\mathrm{GeV}^9$)

| Mass ($J^{PC}$) | State | $\langle \mathcal{O}_{\bar{3}3} \rangle$ | $\langle \mathcal{O}_{6\bar{6}} \rangle$ | $\langle \mathcal{O}_{\mathrm{mix}} \rangle$ | $\Gamma_{\gamma\gamma}$ (keV) |
|---|---|---|---|---|---|
| 6435 $(0^{++})$ | 1s | 0.01323 | 0.00794 | 0.010 | 0.106 |
| 6542 $(0^{++})$ | 1s | 0.02152 | 0.00488 | -0.010 | 0.245 |
| 6849 $(0^{++})$ | 2s | 0.02078 | 0.02605 | 0.023 | 0.149 |
| 6940 $(0^{++})$ | 2s | 0.06234 | 0.00868 | -0.023 | 0.688 |
| 6543 $(2^{++})$ | 1s | 0.01442 | — | — | 0.088 |
| 6928 $(2^{++})$ | 2s | 0.03546 | — | — | 0.217 |

- Mixing term enters with different SDC weight $\Rightarrow$ constructive/destructive interference in decay width.